

# ChemComm

Accepted Manuscript



This is an *Accepted Manuscript*, which has been through the Royal Society of Chemistry peer review process and has been accepted for publication.

*Accepted Manuscripts* are published online shortly after acceptance, before technical editing, formatting and proof reading. Using this free service, authors can make their results available to the community, in citable form, before we publish the edited article. We will replace this *Accepted Manuscript* with the edited and formatted *Advance Article* as soon as it is available.

You can find more information about *Accepted Manuscripts* in the [Information for Authors](#).

Please note that technical editing may introduce minor changes to the text and/or graphics, which may alter content. The journal's standard [Terms & Conditions](#) and the [Ethical guidelines](#) still apply. In no event shall the Royal Society of Chemistry be held responsible for any errors or omissions in this *Accepted Manuscript* or any consequences arising from the use of any information it contains.

Journal Name

COMMUNICATION

www.rsc.org/

Received 00th January 20xx,  
Accepted 00th January 20xx

DOI: 10.1039/x0xx00000x

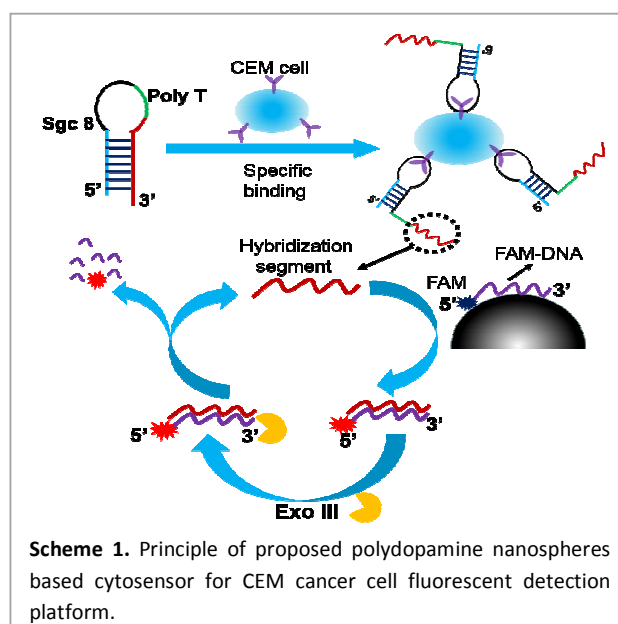
## Polydopamine nanosphere based highly sensitive and selective aptamer cytosensor with Enzyme amplification

 Daoqing Fan<sup>a</sup>, Changtong Wu<sup>ac</sup>, Kun Wang<sup>ac</sup>, Xiaoxiao Gu<sup>ac</sup>, Yaqing Liu<sup>ab\*</sup> and Erkang Wang<sup>a\*</sup>

With CCRF-CEM as model cell, highly sensitive and selective cytosensor was developed by taking advantage of polydopamine nanospheres for the first time. Strategies of aptamer/membrane protein recognition and Exonuclease III assisted cycle amplification were used for improving selectivity and sensitivity. The detection of limit reaches as low as 15 cells/mL.

According to the report presented by the International Agency for Research on Cancer in 2014, about one-eighth death is attributed to cancer or cancer-triggered diseases. Cancer is growing at a striking rate and has been the main pathogenic factor in 21<sup>st</sup> century. Cancer diagnosis and therapy at an early age is critical for improving cure rate, which has aroused great interests of scientists. Among many kinds of cancers, human acute leukemia posed great threats on people's health and life as a result of its high pathogenic rate. It has been reported that it accounts for 10%–15% of pediatric ALL (T-cell acute lymphoblastic leukemia) cases and 25% of adult ALL cases.<sup>1</sup> Hence, it is critical to develop efficient methods for highly sensitive and selective detection of CCRF-CEM cancer cells (T-cell, human acute lymphoblastic leukemia cell line).<sup>2</sup>

Aptamers (Ap) which have great advantages (such as high binding affinity and specificity, controllable structures) over antibody, have been widely used for variable targets detection (cancer cells, protein, ATP and so on) in recent years. By taking advantage of the overexpressed membrane protein (PTK7) on CCRF-CEM cancer cells and its aptamer (sgc8) selected by Tan's group,<sup>3,4</sup> many works have been done for cell imaging, cell detection and other applications. Among those, several fluorescent cytosensors have been developed for the detection of CCRF-CEM cells as for the low background and remote reading ability.<sup>5–8</sup> Except those fluorescent detection



platforms, other methods also have been applied to the detection of CCRF-CEM cells, such as electrochemical or colorimetric strategy.<sup>1, 9–16</sup> The developed platforms usually require multiple modification steps, dual-labelled aptamers, and modified with aptamer conjugated noble metal nanoparticles for conductivity enhancement, signal amplification or taking advantage of noble metal nanoparticles' plasmonic property. It is worthy to note that the used Ag nanoclusters and noble metal nanoparticles could not degrade in organism, which restricts the further application in the early diagnosis of cancer. Therefore, further investigation on constructing novel strategy for highly sensitive and selective cell detection is still required.

It has been reported that polydopamine presents excellent biocompatibility and could biodegrade in organism though metabolism<sup>17</sup> and is usually used as capping or phototherapeutic agent.<sup>18–20</sup> Facile-synthesized and low cost polydopamine nanospheres (PDs) has been widely applied in biomolecules detection such as ATP<sup>21</sup>, miRNA<sup>22</sup> and DNA<sup>23</sup> due to its efficient fluorescence quenching ability. To the best of our knowledge, PDs

<sup>a</sup> State Key Laboratory of Electroanalytical Chemistry, Changchun Institute of Applied Chemistry, Chinese Academy of Sciences, Changchun, Jilin, 130022, P.R. China, University of Chinese Academy of Sciences, Beijing, 100039, China

<sup>b</sup> Key Laboratory of Food Nutrition and Safety (Tianjin University of Science and Technology), Ministry of Education, Tianjin, 300457, P. R. China.

<sup>c</sup> Department of Chemistry and Environmental Engineering, Changchun University of Science and Technology, Changchun, China.

Corresponding authors: yaqingliu@tust.edu.cn; ekwang@ciac.ac.cn, Tel: +86-22-60912484; +86-431-85262378; Fax: +86-431-85689711.

Electronic Supplementary Information (ESI) available: Figure S1–S6. See DOI: 10.1039/x0xx00000x

has not been used for the detection of cancer cells. Herein, for the first time, we constructed a fluorescence cytosensor for highly sensitive and selective detection of CCRF-CEM cancer cells. Strategies of aptamer/membrane protein recognition and Exo III assisted cycle amplification were used to enhance the selectivity and sensitivity.

In our investigation, PDs are synthesized according to a previous report.<sup>24</sup> Learned from SEM image, **Figure 1A**, after self-polymerization of dopamine, monodisperse PDs are obtained with a diameter of about 260 nm. As shown in the IR spectra (**Figure 1B**), characteristic peaks of dopamine between  $1700\text{cm}^{-1}$  to  $400\text{cm}^{-1}$  has disappeared after polymerization, which are consistent with previous report.<sup>24</sup> To validate the fluorescence quenching ability of the synthesized PDs, PDs with different concentrations are added into solution containing 100nM FAM-labelled DNA strand (FAM-DNA), (See **Figure S1 in SI**). A quenching efficiency of 99.15% is reached on the addition of 0.30mg/mL PDs into the FAM-DNA solution. To perform the experiment at optimized conditions, optimization experiments were conducted (See **Figure S2, S4 and S5 in supporting information (SI)**).

**Scheme 1** outlines the principle of the CCRF-CEM cancer cell detection strategy. A molecular beacon is designed as the initial platform, containing three fragments, a sgc8 region that can specifically interact with PTK7 (strand-sgc8, blue and black segments), a poly-thymine (poly-T) DNA spacer (green segment) and a hybridization region (red segment) to hybridize with FAM-labelled DNA strand (FAM-DNA) which is anchored on PDs. The 3' terminus of the molecular beacon is extended with four thymine bases to prevent the aptamer from cleaving by Exo III. In the absence of CCRF-CEM cell, the aptamer's structure is stem-looped with high stability as a result of the hybridization between the blue and red segments. After incubating in CCRF-CEM cells suspension, sgc8 segment would bind PTK7 protein tightly and form cell/Ap complex, resulting in the conformation change of the molecular beacon and liberating the hybridization region (red segment of the Ap). For the detection of cancer cell, FAM-DNA is premixed with suitable volume of PDs, producing FAM-DNA/PDs complex. A low fluorescence background is detected due to the fluorescence resonance energy transfer (FRET) between FAM and PDs. When the FAM-DNA/PDs is added into the cell/Ap complex, the exposed red segment would hybridize with FAM-DNA to form duplex. The fluorescence of FAM is then restored due to the stripping of the

formed duplex from PDs. To improve the sensitivity, Exo III is introduced to activate next amplification round. It has been reported that the activity of Exo III on ssDNA is limited and prefer to blunt or recessed 3'-terminus.<sup>25</sup> In our design, the recessed 3'-terminus of FAM-DNA is exposed after forming duplex with restructured molecular beacon. The Exo III enzyme then can play function to cleave it, releasing the complex of cells/Ap. The released complex would bind FAM-DNA on PDs again and start a new cycle of releasing signal reporter, which leads to significant signal amplification.

The specificity of the molecular beacon probe to PTK 7 protein is testified firstly. The 5'-terminus and 3'-terminus of the molecular beacon are labelled with FAM and BHQ1, respectively. To bring the quencher BHQ1 and the fluorophore FAM together, 8 bases at 3' terminus of the dual-labelled molecular beacon (Label-ap DNA) used here are shorter than that of the aptamer part used for the cancer cell detection (**Table S1**), producing a very low fluorescence signal. After incubating with standard PTK7 protein, an obvious enhanced fluorescence intensity could be obtained than that caused by the same amount of control sample BSA (bovine serum albumin), indicating the high specificity of the aptamer towards PTK7 protein, **Figure 2A**. Additionally, a random dual-labeled hairpin probe (Random probe strand) is also utilized to testify the specificity of PTK 7 protein to the probe, **Figure S2B**. Secondly, the feasibility of the developed strategy for target cells is validated from two sides. On the one side, the reaction of molecular beacon with CCRF-CEM cancer cells is validated. After incubation with CCRF-CEM cells, an obvious fluorescence enhancement is monitored since the configuration change of the molecular beacon results in the far away of the FAM from the BHQ1, which proves the successful binding of aptamer probe with PTK7 protein. On the other side, experiments are conducted to validate the reaction of CCRF-CEM cells/Ap complex with FAM-DNA/PDs. As shown in **Figure 2B**, a very low fluorescence background is monitored after mixing PDs with FAM-DNA (a) and also in the presence of PDs, FAM-DNA and Exo III (b). While, after adding CCRF-CEM cells/Ap into the mixture of PDs and FAM-DNA, an obvious fluorescence recovery could be obtained (c). After adding 25U Exo III into the system, the fluorescence signal

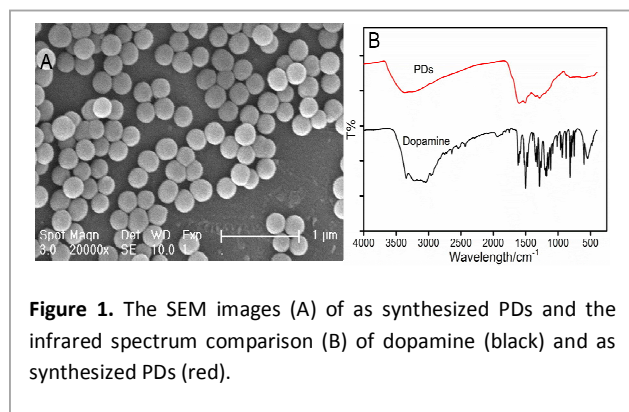


**Figure 1.** The SEM images (A) of as synthesized PDs and the infrared spectrum comparison (B) of dopamine (black) and as synthesized PDs (red).

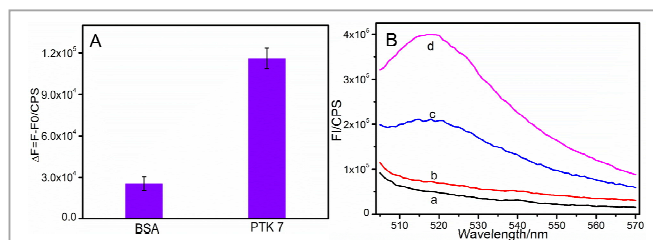
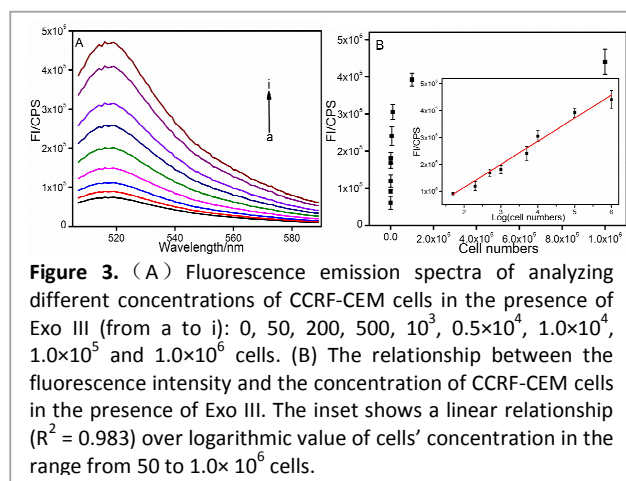


**Figure 2.** (A) Comparison of the fluorescence intensity produced by same amount of BSA, PTK7 using the aptamer probe, where F and F<sub>0</sub> are fluorescence intensities of FAM in the presence and absence of different samples, respectively. The reaction solution contained 100nM Label-ap DNA. Error bars were estimated from three replicate measurements. (B) Fluorescence spectrum of 100nM FAM-strand in the presence of PDs (B, a); PDs+25U Exo III (B, b); PDs+complex of  $1.0 \times 10^5$  cells/Ap (B, c); PDs+complex of  $1.0 \times 10^5$  cells/Ap+25U Exo III (B, d).

is significantly enhanced (d). The results prove the feasibility of the proposed strategy.

For the cancer cell detection, we first studied different concentrations of CCRF-CEM cells in the absence of Exo III (Figure S6). A LOD of 218 cells/mL is obtained according to the calculation of 3 times the standard deviation of background signal. To improve the sensitivity, Exo III is introduced for signal amplification shown in Figure 3. The fluorescence exhibits dramatic enhancement in contrast with enzyme-free condition (Figure S6). Calibration curve of fluorescence intensity at 520 nm as a function of logarithmic value of cells' concentration is shown in the inset of Figure 3B. Linear relationship between fluorescence intensity and the concentration of cells could be obtained in the range from 50 to  $1.0 \times 10^6$  cells/mL ( $R^2=0.983$ ), resulting in a LOD of 15 cells/mL according to the calculation of 3 times the standard deviation of background signal, which is about 15-fold lower than the enzyme-free assay.



Differentiating target cancer cell from different cancer cell types is of critical for cancer diagnosis and therapy.<sup>26</sup> Due to the high affinity of aptamer to the target membrane protein, the aptamer-based cytosensors usually present excellent selectivity. In our investigation, HeLa (cervix adenocarcinoma), MCF-7 (human breast cancer cells) and A549 cancer cells were used to perform control experiment to validate the specificity of the developed cytosensor. It has been reported that HeLa cells have low density expression PTK 7 protein on the membrane's surface,<sup>27</sup> which was confirmed in our investigation as shown in Figure S7. The fluorescence changes indicated the low expression of PTK 7 protein on HeLa, A549, MCF-7 cells. As shown in Figure 4, after the addition of the same concentrations of other kinds of cells, low fluorescence signals are monitored in contrast with the high response triggered by the target cells, which proves the high selectivity of the developed strategy. The possible reason is that the over-expressed PTK7 protein on CCRF-CEM cell membrane is limited or low-expressed on the surface of the non-target cells' membrane. Thus, the non-target cells could not cause configuration change of the designed molecular beacon, leading no signal response. The error bars shown in Figure 3 and Figure 4 are obtained from three independent experiments, respectively, confirming the high repeatability of the developed strategy.

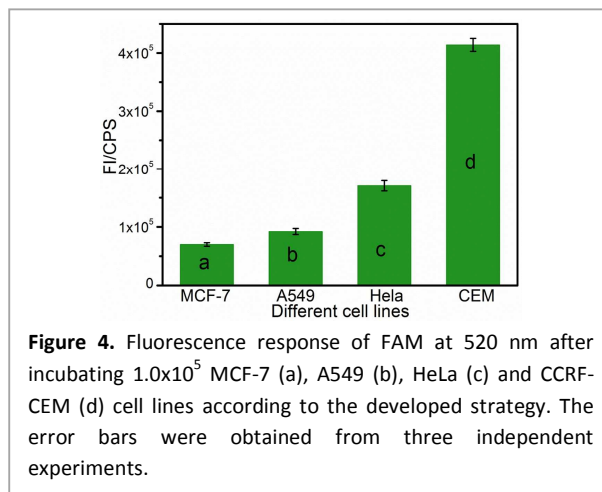


**Figure 4.** Fluorescence response of FAM at 520 nm after incubating  $1.0 \times 10^5$  MCF-7 (a), A549 (b), HeLa (c) and CCRF-CEM (d) cell lines according to the developed strategy. The error bars were obtained from three independent experiments.

In conclusion, based on the efficient fluorescence quenching ability of polydopamine nanospheres and aptamer/membrane protein recognition triggered conformation alteration and Exonuclease III assisted cycle amplification, we for the first time constructed a novel fluorescent cytosensor for highly sensitive and selective detection of CCRF-CEM cancer cells. The detection of limit reaches as low as 15 cells, which is comparable with previous reported methods. The developed strategy presents several advantages. First, the used polydopamine nanospheres is facile-synthesized, low cost and has excellent biocompatibility and biodegradability, which has potential application on early diagnosis of cancer in the future. Second, the developed strategy could be realized rapidly, which is very important for cell detection. Last but not least, the developed strategy could also be used for other cancer cell detection as for its generality.

## Acknowledgements

This work was supported by the National Natural Science Foundation of China (21105095 and 211900040), the State Key Instrument Developing Special Project of Ministry of Science and Technology of China (2012YQ170003), the Instrument Developing Project of the Chinese Academy of Sciences (YZ201203) and the Natural Science Foundation of Jilin Province, China (20130101117JC).

## Notes and references

‡ The authors declare no competing financial interest.

- 1 X. Zhang, K. Xiao, L. Cheng, H. Chen, B. Liu, S. Zhang and J. Kong, *Anal. Chem.*, 2014, **86**, 5567.
- 2 S. Bi, Y. Dong, X. Jia, M. Chen, H. Zhong and B. Ji, *Nanoscale*, 2015, **7**, 7361.
- 3 D. Shangguan, Y. Li, Z. Tang, Z. C. Cao, H. W. Chen, P. Mallikaratchy, K. Sefah, C. J. Yang and W. Tan, *P.Natl.Acad.Sci.USA*, 2006, **103**,

- 11838.
- 4 M. You, G. Zhu, T. Chen, M. J. Donovan and W. Tan, *J. Am. Chem. Soc.*, 2015, **137**, 667.
  - 5 L. Li, Q. Wang, J. Feng, L. Tong and B. Tang, *Anal. Chem.*, 2014, **86**, 5101.
  - 6 L. Yan, H. Shi, X. He, K. Wang, J. Tang, M. Chen, X. Ye, F. Xu and Y. Lei, *Anal. Chem.*, 2014, **86**, 9271.
  - 7 J. Yin, X. He, K. Wang, F. Xu, J. Shangguan, D. He and H. Shi, *Anal. Chem.*, 2013, **85**, 12011.
  - 8 J. Yin, X. He, K. Wang, Z. Qing, X. Wu, H. Shi and X. Yang, *Nanoscale*, 2012, **4**, 110.
  - 9 X. Chen, Y. Wang, Y. Zhang, Z. Chen, Y. Liu, Z. Li and J. Li, *Anal. Chem.*, 2014, **86**, 4278.
  - 10 H. Liu, S. Xu, Z. He, A. Deng and J. J. Zhu, *Anal. Chem.*, 2013, **85**, 3385.
  - 11 X. Chen, Y. He, Y. Zhang, M. Liu, Y. Liu and J. Li, *Nanoscale*, 2014, **6**, 11196.
  - 12 K. Zhang, T. Tan, J. J. Fu, T. Zheng and J. J. Zhu, *Analyst*, 2013, **138**, 6323.
  - 13 C. Pan, M. Guo, Z. Nie, X. Xiao and S. Yao, *Electroanal.*, 2009, **21**, 1321.
  - 14 W. Shan, Y. Pan, H. Fang, M. Guo, Z. Nie, Y. Huang and S. Yao, *Talanta*, 2014, **126**, 130.
  - 15 H. Shi, D. Li, F. Xu, X. He, K. Wang, X. Ye, J. Tang and C. He, *Analyst*, 2014, **139**, 4181.
  - 16 X. Ye, H. Shi, X. He, K. Wang, D. He, L. Yan, F. Xu, Y. Lei, J. Tang and Y. Yu, *Anal. Chem.*, 2015.
  - 17 Y. Liu, K. Ai and L. Lu, *Chem. Rev.*, 2014, **114**, 5057.
  - 18 I. Ocsoy, B. Gulbakan, M. Shukoor, X. Xiong, T. Chen, D. Powell and W. Tan, *ACS Nano*, 2013, **7**, 417.
  - 19 L. Lin, Z. Cong, J. Cao, K. Ke, Q. Peng, J. Gao, H. Yang, G. Liu and X. Chen, *ACS Nano*, 2014, **8**, 3876.
  - 20 Y. Liu, K. Ai, J. Liu, M. Deng, Y. He and L. Lu, *Adv. Mater.*, 2013, **25**, 1353.
  - 21 W. Qiang, X. Wang, W. Li, X. Chen, H. Li and D. Xu, *Biosens. & Bioelectron.*, 2015, **71**, 143.
  - 22 Y. Xie, X. Lin, Y. Huang, R. Pan, Z. Zhu, L. Zhou and C. J. Yang, *Chem. Commun.*, 2015, **51**, 2156.
  - 23 Q. Liu, Z. Pu, A. M. Asiri, A. O. Al-Youbi and X. Sun, *Sensor. Actuat. B-Chem.*, 2014, **191**, 567.
  - 24 W. Qiang, W. Li, X. Li, X. Chen and D. Xu, *Chem. Sci.*, 2014, **5**, 3018.
  - 25 L. Zhang, S. Guo, S. Dong and E. Wang, *Anal. Chem.*, 2012, **84**, 3568.
  - 26 Q. Liu, C. Jin, Y. Wang, X. Fang, X. Zhang, Z. Chen and W. Tan, *NPG Asia Mater.*, 2014, **6**, e95.
  - 27 Chen, Y.; Munteanu, A. C.; Huang, Y. F.; Phillips, J.; Zhu, Z.; Mavros, M.; Tan, W. *Chem.–Eur. J.*, 2009, **15**, 5327–5336

